

PAPER

Generation of subpicosecond pulses due to the development of modulation instability of whispering-gallery-mode wave packets in an optical waveguide with a travelling refractive-index wave

To cite this article: I.O. Zolotovskii *et al* 2018 *Quantum Electron.* **48** 818

View the [article online](#) for updates and enhancements.



IOP | ebooks™

Bringing you innovative digital publishing with leading voices to create your essential collection of books in STEM research.

Start exploring the collection - download the first chapter of every title for free.

Generation of subpicosecond pulses due to the development of modulation instability of whispering-gallery-mode wave packets in an optical waveguide with a travelling refractive-index wave

I.O. Zolotovskii, D.A. Korobko, V.A. Lapin, P.P. Mironov, D.I. Sementsov, A.A. Fotiadi, M.S. Yavtushenko

Abstract. We consider the transformation of a quasi-continuous (with the duration greater than 1 ns) background tunnelling wave of the whispering gallery mode (WGM) type into ultrashort (pico- and subpicosecond) laser pulses, arising due to the development of modulation instability in a cylindrical optical waveguide with travelling refractive-index wave. It is shown that the peak power of the generated laser pulses can exceed the power of the background WGM by a few orders of magnitude.

Keywords: laser pulses, whispering gallery modes, modulation instability, travelling wave, refractive index.

1. Introduction

Surface waves of the whispering gallery mode (WGM) type, in spite of their long history [1], remain to be interesting for researchers in various fields of physics. The WGMs arise in axially symmetric systems and are formed at the curved interfaces between two media. Electromagnetic WGMs can be detected, e.g., in dielectric waveguides of spherical, spheroidal, toroidal, or cylindrical shape [2–4]. In the latter case, such wave packets propagate near the surface of a silica waveguide cylinder along a helix with constant pitch, due to which they are referred to as tunnelling modes [5]. Among the specific features of such helix waves, an important circumstance is that their longitudinal (along the waveguide axis) group velocity can be arbitrarily small relative to the speed of light in vacuum [6, 7].

In the present paper, we consider the transformation of a quasi-continuous (with the duration above 1 ns) background tunnelling wave of the WGM type into ultrashort (pico- and subpicosecond) laser pulses, formed due to the development of modulation instability (MI) in the cylindrical optical waveguide with a travelling refractive-index wave (TRIW). It is shown that the peak power of the generated laser pulses can exceed the power of the background WGM by a few orders of magnitude.

I.O. Zolotovskii, D.A. Korobko, V.A. Lapin, P.P. Mironov, D.I. Sementsov, M.S. Yavtushenko Ulyanovsk State University, ul. L. Tolstogo 42, 423017 Ulyanovsk, Russia; e-mail: rafzol.14@mail.ru; A.A. Fotiadi Ulyanovsk State University, ul. L. Tolstogo 42, 423017 Ulyanovsk, Russia; Université de Mons, 20, place du Parc, B7000 Mons, Belgium

Received 17 May 2018; revision received 25 June 2018
 Kvantovaya Elektronika 48 (9) 818–822 (2018)
 Translated by V.L. Derbov

2. Equations for the surface tunnelling wave field

When the light is injected into a cylindrical waveguide at a certain angle with the cylinder generatrix, the surface wave generally propagates along a helix trajectory [3, 5–8]. The longitudinal component of the wave vector of such a wave is $k_z = (k^2 - k_r^2)^{1/2}$, where $k = k_0 n(\omega)$: $k_0 = \omega/c$ is the wave number in vacuum; $n(\omega)$ is the refractive index of the optical waveguide material; and k_r is the transverse (radial) component of the wave vector. If the direction of the wave injection into the optical waveguide is sufficiently close to the normal (with respect to the generatrix), then the wave propagation along the waveguide axis is essentially decelerated up to zero velocity values [9, 10].

Below we consider the case of a surface wave slowly tunnelling (with the velocity $V_z \ll c$) along the longitudinal axis z of the waveguide (this is possible if $k_z \ll k - k_r$) (Fig. 1). In this case, the electric field of the wave can be presented as

$$E(z, r, t, \varphi) = A(z, t)\Phi(r, z, \varphi)\exp\left[i\omega t - i\int_0^z k_z(z)dz\right], \quad (1)$$

where $A(z, t)$ is the slowly varying amplitude that describes the longitudinal distribution of the tunnelling wave field; and $\Phi(r, z, \varphi)$ is the function that defines the radial and azimuthal dependence of the field in the optical waveguide. For exam-

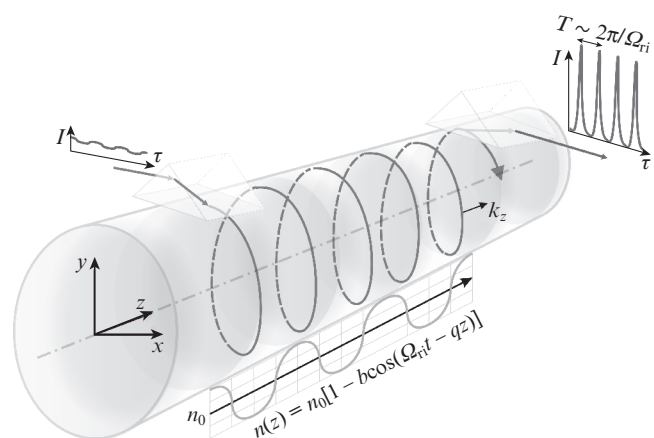


Figure 1. Trajectory of the ray injected into the cylindrical optical waveguide and representing the wave of the whispering gallery mode type.

ple, in the quasi-linear approximation for a homogeneous cylindrical waveguide with the radius a at $r \leq a$ for the azimuthal mode of the m th order this function can be written as [9, 10]

$$\Phi_m(r, \varphi) = \Phi_0 Ai[\sqrt{2m^2(1-r/a) - \xi_m}] \exp(im\varphi), \quad (2)$$

where $Ai[\dots]$ is the Airy function of the first kind; ξ_m is the appropriate root of the Airy function [9, 11]; and φ is the angle between the x axis and the radius vector r . For $r > a$ we assume $\Phi_m(r, \varphi) \rightarrow 0$.

The dynamics of the temporal envelope of the wave packet (WP) in this optical waveguide is described by the nonlinear Schrödinger equation [12]

$$\frac{\partial A}{\partial z} + V_z^{-1} \frac{\partial A}{\partial t} - iD_z \frac{\partial^2 A}{\partial t^2} + iR_z |A|^2, \quad A = 0, \quad (3)$$

where the longitudinal velocity of the wave, the group velocity dispersion (GVD), and the waveguide nonlinearity are defined as

$$V_z(z) \approx \gamma \frac{\partial \omega}{\partial k}, \quad D_z(z) \approx \frac{1}{\gamma} \frac{\partial^2 k}{\partial \omega^2}, \quad \text{and} \quad R_z \approx n^{(2)} k / (\gamma S_{\text{eff}}), \quad (4)$$

respectively. Here $\gamma(z) = (1 - k^2/k^2)^{1/2}$ is the parameter of the tunnelling wave longitudinal deceleration; $n^{(2)}$ is the material cubic nonlinearity coefficient; and

$$S_{\text{eff}}(m) = \left(\int_{-\pi}^{\pi} \int_0^{\infty} r |\Phi(r, \varphi, m)|^2 d\varphi dr \right)^2 \times \left(\int_{-\pi}^{\pi} \int_0^{\infty} r |\Phi(r, \varphi, m)|^4 d\varphi dr \right)^{-1} \quad (5)$$

is the effective area of the surface mode.

3. Interaction of a tunnelling wave with a TRIW

Assume that the TRIW propagates in the optical waveguide. To implement it one can, e.g., arrange modulators of the refractive index along the waveguide axis [6–8]. Under the action of modulators, a travelling wave will be produced in the optical waveguide, in which the refractive index of the medium varies as

$$n(t, z) = n_0 [1 - b \cos(\Omega_{\text{ri}} t - qz)], \quad (6)$$

where Ω_{ri} is the modulation frequency; $q = 2\pi/\Lambda$ is the wave number of the TRIW; Λ is the period of spatial inhomogeneity; $V_a = \Omega_{\text{ri}}/q$ is the velocity of TRIW ‘movement’; $b = \Delta n/n_0$ is the modulation depth; and Δn is the maximal change of the refractive index. Note that the TRIW can be also implemented in an optical waveguide by exciting an acoustic wave. The phase velocity of such wave $V_a \approx \gamma c/n \approx 6000 \text{ m s}^{-1}$. Thus, in a silica waveguide with the standard value of $n \approx 1.5$ the matching of the tunnelling wave packet and the TRIW requires $\gamma \approx 3 \times 10^{-5}$. The modulation depth b in this case can attain 3×10^{-4} [13].

When $V_z \approx V_a$, the tunnelling surface wave of the WGM type and the TRIW experience strong resonance coupling. In this case, the equation describing the dynamics of the temporal envelope of the tunnelling WP in the coordinate frame travelling with the wave packet can be presented in the form

$$\frac{\partial A}{\partial z} - iD_z \frac{\partial^2 A}{\partial \tau^2} + iR_z |A|^2 A = ikb\gamma^{-1} \cos[\Omega_n(\tau - \delta\tau)] A, \quad (7)$$

where the parameter $\delta\tau = (V_a^{-1} - V_z^{-1})z$ characterises the time detuning related to the difference of the wave packet group velocity and the TRIW velocity. As shown by numerical simulation, Eqn (7) sufficiently well describes the dynamics of the wave of the classical WGM type in the case when this wave is ‘carried’ by the TRIW with the modulation depth $b = \Delta n/n_0$ no smaller than 10^{-4} .

One can implement the strong matched coupling of the electromagnetic wave and the TRIW, described by Eqn (6), not only using the waves slowly tunnelling along the optical waveguide axis, but also using a waveguide coiled on a cylinder with the diameter $d > a$, along the axis of which the TRIW is excited [14–16]. The velocity component of the electromagnetic wave along the cylinder axis is determined by the cylinder dimensions and the winding angle $\kappa \approx h/2\pi a$ that determines the deceleration, where h is the pitch of the waveguide helix. In this case, the inevitably arising ‘bending’ losses of the densely coiled optical waveguide can be compensated for by using amplifying optical waveguides and side pumping.

4. Regime of superpulse formation, numerical analysis

The study of the MI development and formation of picosecond pulses with a peak power exceeding the intensity of background radiation by orders of magnitude will be performed basing on the numerical solution of Eqn (7) using the split-step Fourier method (SSFM) [12]. Let us assume that the signal entering the optical waveguide is a weakly modulated quasi-continuous one expressed as

$$A(0, \tau) = \sqrt{P_0} [1 + \zeta \cos(\Omega_{\text{mod}} \tau)], \quad (8)$$

where $P_0 = |A_0|^2$ is the power of the input radiation; ζ is the modulation depth; and Ω_{mod} is the modulation frequency of the wave packet.

Figure 2 illustrates the dynamics of the MI development and the formation of one of a sequence of superpulses (SPs) from the initially continuous pump wave. For numerical modelling the following values of parameters have been chosen: $\gamma D_z = -10^{-26} \text{ s}^2 \text{ m}^{-1}$, $P_0 = 0.1 \text{ W}$, $\zeta = 10^{-3}$, $\beta = 10^6 \text{ m}^{-1}$, $\gamma = 4 \times 10^{-5}$, $\Omega_{\text{mod}} = 10^{12} \text{ s}^{-1}$, $\Omega_{\text{ri}} = 10^9 \text{ s}^{-1}$, $\Delta n = 10^{-4}$.

The picture of SP formation as a result of the MI development (both spontaneous and induced) can be presented as follows: at first the induced MI develops and the high-frequency train of pulses (breathers) appears with the repetition rate $\Omega_{\text{max}} = \sqrt{R_z P_0 / |D_z|}$ and the duration of individual pulse $\tau_p \approx 2\pi / \Omega_{\text{max}}$. The harmonic perturbation gain increment at this stage of MI is given by the expression [12, 17–19]

$$g(z, \omega) = 2|\Omega \gamma D_z| \sqrt{2P_0 R_z / D_z - \Omega^2}, \quad (9)$$

where $\Omega = \omega - \omega_0$, ω is the frequency of harmonic perturbation, and ω_0 is the frequency of the input wave packet.

The next stage consists in the pulling of breathers towards the regions of the maximal refractive index of the TRIW and the formation of a high-energy WP (bunch) with the energy $W_s \sim 2\pi P_0 / \Omega_{\text{ri}}$. Thus, with a good degree of accuracy for the chosen frequency and depth of modulation of the initially continuous wave with the power 100 mW, the peak power (P_{max}) of the SP formed at the optical waveguide length z_s ,

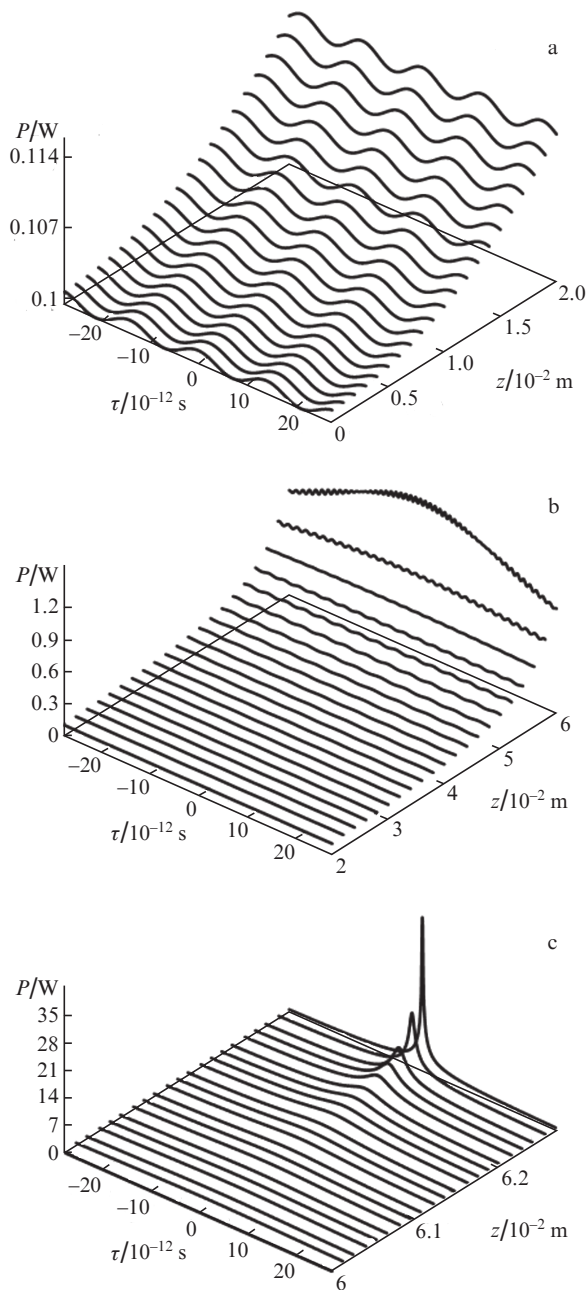


Figure 2. Dynamics of the MI development and the formation of one of a sequence of ultrashort pulses from the initially continuous wave for $\gamma D_z = 10^{-26} \text{ s}^2 \text{ m}^{-1}$, $P_0 = 0.1 \text{ W}$, $\gamma R_z = 10^{-2} (\text{W m})^{-1}$, $\beta = 10^6 \text{ m}^{-1}$, $\gamma = 4 \times 10^{-5}$, $\Omega_{ri} = 10^9 \text{ s}^{-1}$, $\Delta n = 10^{-4}$.

determined by the relation $z_s \sim 1/\Omega_{ri} \approx 6 \text{ cm}$, exceeds 20 kW, and its duration $\tau_s \sim W_s/P_{\text{max}} \sim 2\pi P_0/(\Omega_{ri} P_{\text{max}})$ tends to the value smaller than 10^{-13} s . In this case, the smaller the repetition rate of the breathers, the higher the peak power (the smaller the repetition rate, the greater the energy collected by the SP due to the coherent summation of the energy of breathers generated during the time $T \approx 2\pi/\Omega_{ri}$ and concentrated in one SP).

For the above parameters, Fig. 3 presents the formation dynamics for the entire sequence of SPs (only three pulses are shown). It is seen that as z approaches z_s ($z \leq z_s$), the SP peak power rapidly increases due to the coherent summation of breathers formed by the MI development. Note that the formation of a superhigh-power pulse occurs in exclusively small

‘longitudinal scale’ (significantly smaller than 1 mm). For $z > z_s$ the propagating radiation becomes chaotic and the WP decays into noise components due to nonlinear effects and higher-order dispersion effects. Generally, the further analysis of SP dynamics requires considering dispersion and nonlinear effects of higher orders.

The authors of Refs [15, 19] showed that at the path lengths $z \approx z_s$, the WP (Gaussian-shaped frequency modulated pulse) described by Eqn (7) under the conditions of anomalous GVD experiences strong modulation leading to ultrafast variation of all basic parameters (duration, amplitude, chirp, pulse phase). Basing on the results of these papers, one can obtain an approximate expression for the parameter z_s that provides good agreement with the results of numerical solution of Eqn (7):

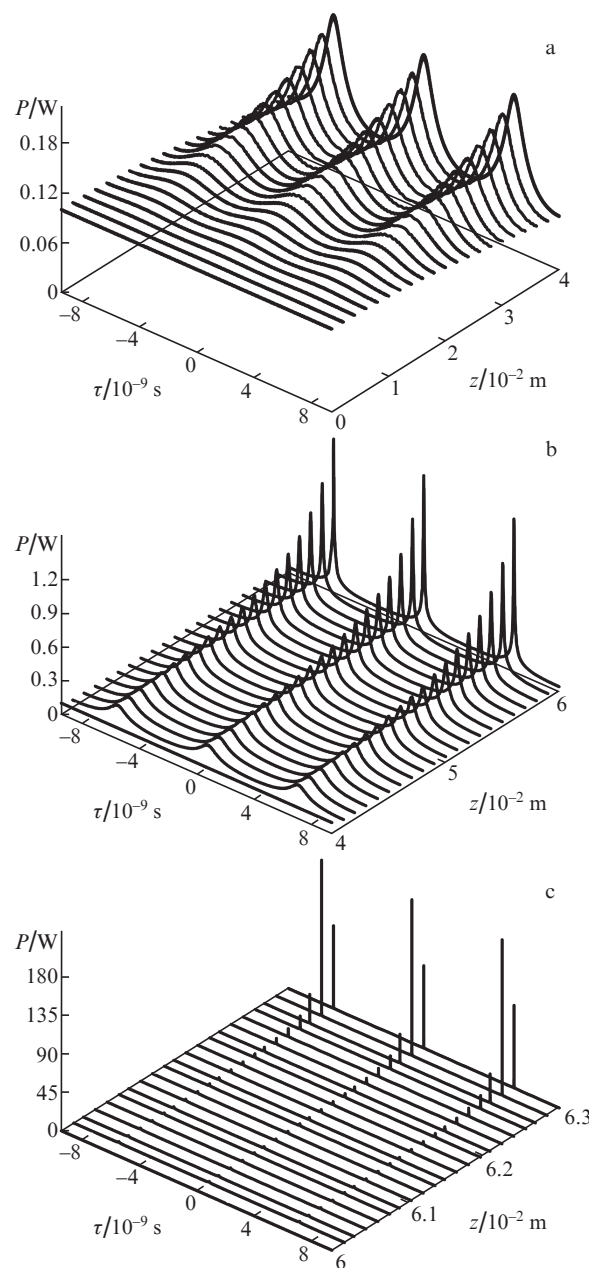


Figure 3. Transformation of the quasi-continuous wave into a sequence of ultrashort pulses (the values of parameters are the same as in Fig. 2).

$$z_s \approx \pi |8bk\gamma^{-1}D_2\Omega_{ri}^2|^{-1/2}. \quad (10)$$

As shown below, at this length the SP is produced as a result of the development of the modulation instability regime.

Figure 4 presents the formation dynamics for a sequence of superpulses (only three of them are shown) at the above parameters and two values of the TRIW modulation frequency: $\Omega_{ri} = 10^9$ and 10^{10} s^{-1} . The analysis has shown that the duration (τ_s) of the SP generated in optical waveguides with the modulation frequency lying within the considered range (for the same values of other parameters) is nearly similar and amounts to $\sim 10^{-13} \text{ s}$. The length of SP formation is inversely proportional to the modulation frequency [which follows from Eqn (9)]; we obtained $z_s \approx 6 \text{ cm}$ for $\Omega_{ri} = 10^9 \text{ s}^{-1}$ and $z_s \approx 6 \text{ mm}$ for $\Omega_{ri} = 10^{10} \text{ s}^{-1}$. Thus, the frequency and the depth of modulation do not essentially affect the character of the formation of the SP sequence (duration, amplitude, repetition rate). The weak dependence of the SP sequence formation dynamics on the modulation depth ζ indicates the possibility of the spontaneous MI development.

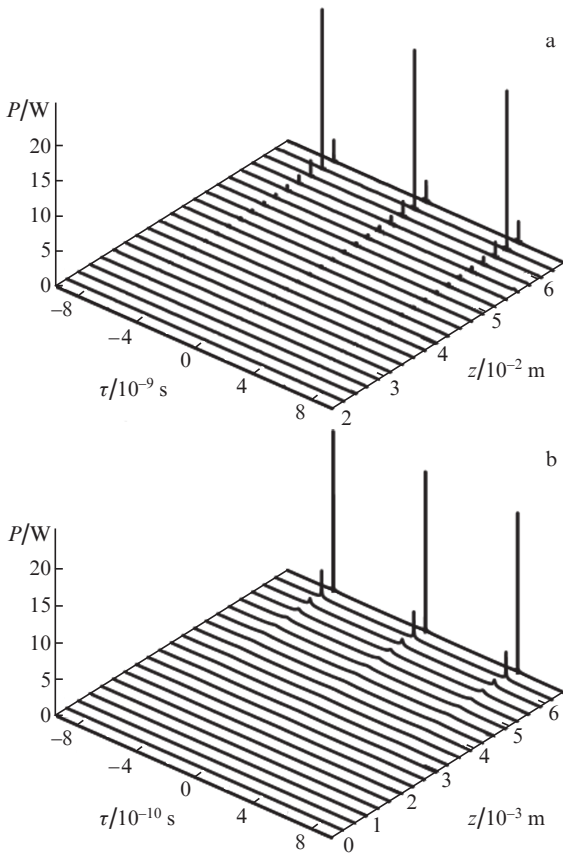


Figure 4. Dynamics of the formation of a sequence of ultrashort pulses at the TRIW modulation frequencies $\Omega_{ri} = 10^9$ and 10^{10} s^{-1} (the rest parameters are the same as in Fig. 2).

Figure 5 presents the dependences of the maximal SP power on the optical waveguide length, calculated for the modulation frequency $\Omega_{ri} = (1, 5, 6, 7, 8, 9, 10) \times 10^9 \text{ s}^{-1}$. It is seen that with the growth of Ω_{ri} the maximal SP power decreases. For the SP energy, the relation $W_1/W_2 \approx \Omega_{ri2}/\Omega_{ri1}$ can be considered valid with good degree of accuracy.

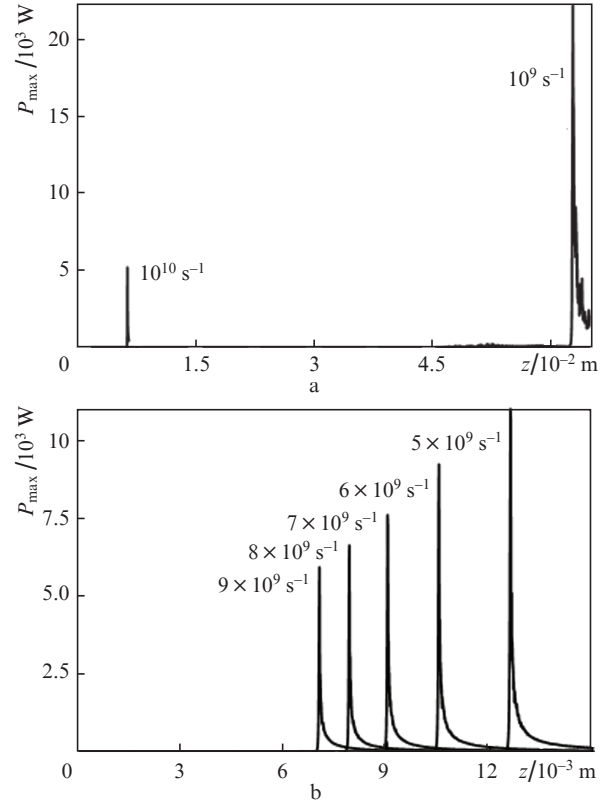


Figure 5. Dependences of the superpulse maximal power on the optical waveguide length for the TRIW modulation frequency (a) $\Omega_{ri} = 10^9$ and 10^{10} s^{-1} and (b) $\Omega_{ri} = (5, 6, 7, 8, 9) \times 10^9 \text{ s}^{-1}$.

Note in conclusion that besides the considered implementation of matched coupling of the TRIW and the wave packet injected into the optical waveguide, the electrooptic modulation can be used in principle (e.g., as proposed in Refs [20–22]). However, the acoustooptical coupling of the slow tunnelling wave and the acoustic TRIW is nowadays the most technologically developed method of obtaining the effects discussed in the paper.

5. Conclusions

We have considered the development of the modulation instability of tunnelling waves in the optical waveguide with the TRIW. It is shown that when the tunnelling wave velocity along the optical waveguide axis equals that of the TRIW, in the vicinity of the characteristic length z_s the super-strong modulation of the wave packet takes place and the pulses having pico- and subpicosecond duration are formed with the repetition rate, equal to the TRIW modulation frequency Ω_{ri} . The peak power of generated pulses can exceed the power of the weakly modulated background radiation injected into the waveguide by a few orders of magnitude. It is found that the quasi-continuous radiation with the power 1 W can be used to generate subpicosecond pulses with the peak power essentially exceeding 10 kW. The formation of superhigh-power pulse occurs in exclusively small ‘spatial scales’, significantly smaller than 1 mm.

Acknowledgements. The work was supported by the Ministry of Education and Science of the Russian Federation (Project

No.14.Z50.31.0015, State Task 3.3889.2017PCh) and the Russian Science Foundation (Project No. 16-42-02012).

References

1. Rayleigh, Lord. *Phil. Mag.*, **20**, 1001 (1910).
2. Torchigin V.P. *Quantum Electron.*, **25** (5), 484 (1995) [*Kvantovaya Elektron.*, **22** (5), 509 (1995)].
3. Karakantzas G., Dimmick T.E., Birks T.A., Le Roux R., Russell St.J. *Opt. Lett.*, **26**, 1137 (2001).
4. Snyder A.W., Love J. *Optical Waveguide Theory* (Erice, Italy: Springer Science & Business Media, 2012).
5. Ivanov O.V., Nikitov S.A., Gulyaev Yu.V. *Phys. Usp.*, **49** (2), 167 (2006) [*Usp. Fiz. Nauk.*, **167** (2), 175 (2006)].
6. Sychugov V.A., Magdich L.N., Torchigin V.P. *Quantum Electron.*, **31** (12), 1089 (2001) [*Kvantovaya Elektron.*, **31** (12), 1089 (2001)].
7. Sychugov V.A., Torchigin V.P., Tsvetkov M.Yu. *Quantum Electron.*, **32** (8), 738 (2002) [*Kvantovaya Elektron.*, **32** (8), 738 (2002)].
8. Torchigin V.P., Torchigin S.V. *Quantum Electron.*, **33** (10), 913 (2003) [*Kvantovaya Elektron.*, **33** (10), 913 (2003)].
9. Sumetsky M. *Opt. Lett.*, **29** (1), 8 (2004).
10. Suchkov S.V., Sumetsky M., Sukhorukov A.A. *Opt. Lett.*, **40**, 3806 (2015).
11. Feduryuk M.V. *Eiri funktsii*. V sb. *Matematicheskaya entsiklopediya*. Pod red. I.M. Vinogradova (*Airy Functions*. In: *Mathematical Encyclopaedia*. Ed. by I.M. Vinogradov) (Moscow: Sov. entsiklopediya, 1985) Vol. 5.
12. Agrawal G. *Nonlinear Fiber Optics* (New York: Academic Press, 2007).
13. Goutzoulis A.P., Pape D.R. *Design and Fabrication of Acousto-optic Devices* (New York: Marcel Dekker, 1994) p.68.
14. Torchigin V.P. *Quantum Electron.*, **23** (3), 235 (1993) [*Kvantovaya Elektron.*, **20** (3), 276 (1993)].
15. Zolotovskii I.O., Lapin V.A., Sementsov D.I. *Quantum Electron.*, **46** (1), 39 (2016) [*Kvantovaya Elektron.*, **46** (1), 39 (2016)].
16. Korobko D.A., Okhotnikov O.G., Stoliarov D.A., Sysoliatin A.A., Zolotovskii I.O. *J. Lightwave Technol.*, **33**, 3643 (2015).
17. Zolotovskii I.O., Korobko D.A., Lapin V.A. *Quantum Electron.*, **44** (1), 42 (2014) [*Kvantovaya Elektron.*, **44** (1), 42 (2014)].
18. Korobko D., Okhotnikov O., Zolotovskii I. *J. Opt. Soc. Am. B*, **30**, 237 (2013).
19. Zolotovskii I.O., Korobko D.A., Lapin V.A., Sementsov D.I. *Opt. Spectrosc.*, **121** (2), 256 (2016) [*Opt. Spektrosk.*, **121** (2), 277 (2016)].
20. Bulyuk A.N. *Quantum Electron.*, **22** (10), 948 (1992) [*Kvantovaya Elektron.*, **19** (10), 1018 (1992)].
21. Torchigin V.P. *Quantum Electron.*, **23** (3), 241 (1993) [*Kvantovaya Elektron.*, **20** (3), 283 (1993)].
22. Bulyuk A.N. *Quantum Electron.*, **25** (1), 66 (1995) [*Kvantovaya Elektron.*, **22** (1), 75 (1995)].